# Prediction of Fluid Mixture Transport Properties by Molecular Dynamics<sup>1</sup>.

D. K. Dysthe<sup>2</sup>, A. H. Fuchs<sup>2</sup> and B. Rousseau<sup>2,3</sup>

<sup>&</sup>lt;sup>1</sup> Paper presented at the Thirteenth Symposium on Thermophysical Properties, June 23-27, 1997, Boulder, Colorado, U.S.A.

 $<sup>^2</sup>$  Laboratoire de Chimie Physique des Matériaux Amorphes, Bâtiment 490, Université Paris-Sud, 91405 Orsay Cedex, France

 $<sup>^3</sup>$  To whom correspondence should be addressed

## **Abstract**

Equilibrium molecular dynamics simulations of mixtures of n-decane with methane, ethane and carbon dioxide were performed using the anisotropic united atoms model for n-decane and one and two centre Lennard-Jones models for the light components. The Green-Kubo relations were used to calculate the viscosity, thermal conductivity, inter- and intradiffusion. Viscosities are predicted with a maximum deviation of 30% at low gas concentration and less than 10% deviation at high gas concentration. The viscosity and the thermal conductivity are less sensitive to the cross interactions than the diffusion coefficients that exhibit deviations between different models and with experiments up to 60%.

KEY WORDS: alkanes; carbon dioxide; diffusion; mixtures; molecular dynamics; thermal conductivity; viscosity.

#### 1 Introduction

Knowledge of transport properties of multicomponent gases and oils is of great economical importance both in reservoir modeling, planning of transport and in dimensioning of industrial plants. For mixtures of constituents of dissimilar size, shape and polarity traditional prediction methods for viscosity and thermal conductivity need experimental data to fit mixing rules [1] whereas for diffusion the few existing prediction methods deviate with up to almost an order of magnitude [2]. One possible route to obtaining better prediction is to use molecular dynamics (MD) that can predict thermophysical properties from models of molecular interactions only. Most interaction models proposed have been applied to transport properties at only one or two state points and hardly any transport studies have been performed on mixtures. Two recent studies [3, 4] have, however tried to evaluate four different realistic, flexible models of alkanes at one component fluid states in a more systematic manner. The main criteria for evaluating the models are that they should be 1) simple in order to keep computing time to a minimum, 2) transferable in the sense that the same group parameters can be used for all molecules of the same family, 3) property independent meaning that regressing the parameters for one property should give good predictions of other properties, 4) state independent; the accuracy of prediction should not depend on the temperature, density and composition.

In this work we concentrate on the criteria 3 and 4, the property and state independence. More precisely, we use MD and the Green-Kubo (GK) formalism to study transport coefficients as function of composition at constant temperature and pressure in mixtures of n-decane with methane, ethane and carbon dioxide. These represent mixtures of n-decane with a small spherical and two linear, rigid molecules with different quadrupole moments. We have chosen mixtures of dissimilar molecules because the model interaction parameters regressed in the pure fluid, i.e. in an environment of like molecules, may not be directly transferable to an environment of molecules of different shape, size and interaction types (for instance polarity).

#### 2 Models

As mentioned we will require our models to be simple, transferable and giving predictions that are property and state independent.

For n-decane we use the Padilla and Toxyaerd[5] anisotropic united atom (AUA) model where the  $CH_i$  potential centres are displaced from the carbon atom positions. The bonds are modeled by constraining the distance between adjacent  $CH_i$  groups. This flexible chain model includes bending and torsional motion as well. This ndecane model is the least density and temperature dependent of the currently used flexible UA models[4]. The potential parameters of all the molecular models used in this work are given in Table 1. Methane is modeled as a single LJ potential with parameters given by Möller et al. [6]. Ethane and  $CO_2$  are modeled as two centre LJ (2CLJ) models where the distance between the two centres is constrained. Both ethane and  $\mathrm{CO}_2$  have considerable quadrupole moments (-1.2DÅ and -4.3DÅ respectively). tively) and even though simulated equilibrium properties show reasonable agreement with experiment in a small range of states [7, 8] it is yet unknown to what degree the 2CLJ models satisfy the criteria of property and state independence. The gain in computer time for the 2CLJ model relative to adding a point quadrupole or partial charges (and a third LJ centre for CO<sub>2</sub>) is not decisive for the model choice, the molecules are small and still quite tractable with current workstations. For the pure fluid calculations the models employed in this work are not optimal even though the results in this work shows that the pure fluid transport coefficients are predicted to within the uncertainties. For mixtures of ethane and CO<sub>2</sub> with LJ UA models of alkanes on the other hand, it is clearly computationally faster (by up to an order of magnitude) to treat cross interactions with LJ mixing rules,  $\sigma_{ij} = f(\sigma_{ii}, \sigma_{jj})$  and  $\varepsilon_{ij} = g(\varepsilon_{ii}, \varepsilon_{jj})$ , rather than adding new interaction potentials for the interactions between the quadrupole or partial charges of ethane and CO<sub>2</sub> with polarizable nalkane sites. For the system ethane  $-CO_2$  there is evidence that one may reproduce "non-ideal" effects with the models we have described. Fincham et al.[9] were able to

demonstrate azeotropy of this mixture in qualitative agreement with experimental data only by modifying the Lorentz-Berthelot mixing rules:  $\varepsilon_{ij} = (1 - k_{ij})\sqrt{\varepsilon_{ii}\varepsilon_{jj}}$  with  $k_{ij} = 0.2$  (and  $\sigma_{ij} = (\sigma_{ii} + \sigma_{jj})/2$  as normal). Wang and Cummings[10] reported that using the parameters of Fincham et al., their NEMD simulations of the viscosity of ethane –  $CO_2$  at the density 20 mol  $l^{-1}$  and temperature ranging from 150 to 280K reproduced a plateau region as a function of composition. In the  $CO_2$  – n-decane system we employ both  $k_{ij} = 0.2$  and  $k_{ij} = 0$  to study the effect on the transport coefficients of the attractive cross interactions. For the ethane – n-decane and the methane – n-decane mixtures we use Lorentz-Berthelot mixing rules.

#### 3 Simulation details

We have employed two different MD programs developed independently. The details of the program for workstations[4] (used for methane – n-decane and ethane – n-decane) and that used on a Cray T3E[11] (used for  $CO_2$  – n-decane) will be published separately. Both programs use the RATTLE[12] algorithm to solve the constrained equations of motion. In order to study the property independence of the models we have chosen to use the Green–Kubo (GK) formalism that yields all the transport properties simultaneously; non-equilibrium methods are always property specific. We calculate the viscosity,  $\eta$ , the thermal conductivity,  $\lambda$ , the intradiffusion coefficients,  $D_a$ , and the kinetic interdiffusion coefficients  $D_{12}^K$  by the usual correlation function integrals:

$$\eta = \frac{V}{10k_BT} \int_0^\infty dt \langle \mathbf{P}^{0S}(t) : \mathbf{P}^{0S}(0) \rangle, \tag{1}$$

$$\lambda = \frac{V}{3k_B T^2} \int_0^\infty dt \langle \boldsymbol{J}_q(t) \cdot \boldsymbol{J}_q(0) \rangle, \qquad (2)$$

$$D_a = \frac{1}{3N_a} \int_0^\infty dt \sum_{i \in a} \langle \boldsymbol{v}_i(t) \cdot \boldsymbol{v}_i(0) \rangle$$
 (3)

and 
$$D_{12}^K = \frac{V^2}{3Nw_1w_2m_1m_2} \int_0^\infty dt \langle \boldsymbol{J}_1(t) \cdot \boldsymbol{J}_1(0) \rangle.$$
 (4)

Here V is the system volume, T the temperature,  $\mathbf{P}^{0S}$  the symmetric traceless pressure tensor,  $\mathbf{J}_q$  the heat flux,  $\mathbf{J}_1$  the mass flux of component 1,  $\mathbf{v}_i$  the instantaneous velocity of the centre of mass of molecule i, N the total number of molecules,  $N_a$  the number of molecules of type a,  $w_i$  the mass fraction,  $m_i$  the molecular mass and t the time. We apply the molecular definition of  $\mathbf{P}^{0S}$  and  $\mathbf{J}_q$ . We have not attempted to correct the thermal conductivity for the lack of partial molar enthalpies in the microscopic heat flux definition[13]. The kinetic interdiffusion coefficient  $D_{12}^K$  is connected to the experimentally accessible interdiffusion coefficient  $D_{12} = B_x D_{12}^K$  with a thermodynamic factor  $B_x = \frac{x_1}{RT} \left( \frac{d\mu}{dx_1} \right)_{T,P}$ .

All the simulations were performed with 108 molecules. Each configuration was equilibrated and stabilized at the desired temperature during 1 ns. The production runs were performed for 4 ns in the NVE ensemble with 4 fs time steps. During each run 15 sub averages were saved to disk as basis for statistical analysis. The loss of total energy per nanosecond in an NVE run was never more than 0.3 times the standard deviation of the kinetic energy.

## 4 Results and discussion

We have performed simulations of the methane – n-decane and  $CO_2$  – n-decane systems at 7 compositions and at 6 compositions for the ethane – n-decane system in the range  $x_1$ =0 to 1 (let component 1 be the light component) For methane – n-decane and ethane – n-decane the temperatures were about 333K and densities corresponded to 40 MPa, for the  $CO_2$  – n-decane system temperatures were about 311K and densities corresponded to 27.7 MPa. The densities were obtained from Reamer and Sage[14] for ethane – n-decane, from Reamer et al.[15] for methane – n-decane, from Scaife and Tait for n-decane<sup>1</sup> and from Cullick and Mathis[18] for  $CO_2$  – n-decane. Table 2 contains the results of all the simulations. The statistical

<sup>&</sup>lt;sup>1</sup>The n-decane density used has later been found to correspond to a pressure of 30 MPa.[15, 16] and the results are therefore compared with experiments at the simulated densities or at 30 MPa.

uncertainties are estimated for each single run as the standard deviation of the mean of the 15 sub averages. They are approximately 10% for the viscosity, 10% for the thermal conductivity,  $x_i^{-1/2}$ % for the intradiffusion coefficients  $D_i$  and  $4(x_1x_2)^{-1/2}$ % for the kinetic interdiffusion coefficient  $D_{12}^K$ .

The Figures 1 and 4 show that all the viscosity results have much in common. The methane – n-decane and pure n-decane viscosities displayed in Figure 1 are compared to experimental data from Knapstad et al. [16], the ethane – n-decane viscosities are compared to the empirical correlation of Assael et al.[17] and the  $CO_2$  – n-decane viscosities are compared to the experimental data of Cullick and Mathis [18]. The simulations underestimate the viscosities by up to 30% for n-decane—rich mixtures. At x > 0.5 there is no more any significant deviation. The nature and precision of the simulations are such that we are not able to distinguish between two possible causes of the deviations: 1) The underestimation of the viscosity of n-decane model in the pure fluid at high density. As the gas content increases the density decreases and the n-decane molecules are less important for the viscosity. 2) Poor modeling of the cross interactions (site-site interactions and the total interaction between different molecules) causing a too large fluidity. Some discrimination of these effects may be obtained from the interesting result that for  $CO_2$  – n-decane (Fig. 4) the two curves for  $k_{ij} = 0$  and  $k_{ij} = 0.2$  hardly differ. At  $x_1 = 0.5$  the 13% difference between the two models is not very significant; the errors bars overlap. This shows that the viscosity (and thermal conductivity in Table 2) is virtually independent of details in the attractive site-site cross interaction. The model mixtures employed interpolate the pure component viscosities in a smooth manner and in the case of  $\mathrm{CO}_2-$  n-decane the change in the attractive part of the cross interactions does not alter this behaviour. The cross interaction effect of the different molecular shapes and sizes can still not be discriminated from the underestimation caused by the poor n-decane potential.

In Figures 2 and 3 we compare simulation results of the methane – n-decane and

ethane – n-decane systems with diffusion coefficients from Hafskjold and coll.[2, 19]. The most striking features of the intradiffusion coefficients are the overestimation of  $D_1$  at low gas concentration ( $x_1 < 0.6$ ) and underestimation of  $D_2$  at low n-decane concentration ( $x_1 > 0.6$ ). In the methane – n-decane system the deviation reaches 35% for both methane and n-decane at  $x_1 = 0.093$  and  $x_1 = 0.907$ , respectively. Ethane diffusion is overestimated by as much as 57% at  $x_1 = 0.398$  and n-decane underestimated by 17% at  $x_1 = 0.87$ . The large deviations in  $D_i$  at low concentration of type i in the mixture is a clear sign that the cross interactions are not well represented. The interdiffusion coefficient in the  $CO_2$ – n-decane system is very much affected by the change in  $k_{ij}$  (see Fig. 4). The reduction in attractive cross interaction makes  $D_{12}^K$  increase over the whole composition range with a maximum increase of 55% at  $x_1 = 0.648$ . The diffusion coefficients are, in contrast to the viscosity and thermal conductivity, sensitive to the attractive cross interactions as well as the steric effects of shape and size and the imprecision of the pure n-decane potential.

For methane – n-decane we have included three experimental points for  $D_{12}$ . In order to compare with the simulations we have calculated  $B_x$  using the Peng-Robinson equation of state setting the binary interaction parameter to 0.0265. At  $x_1 = 0.093$  where  $B_x = 0.98$  the difference between simulation and experiment is only 4%. At  $x_1 = 0.907$  the  $D_{12}$  deduced from simulation is 60% too low. Because of the incorrect analytical form of the equation of state on approaching the critical point one must expect  $B_x$  and thus  $D_{12}$  from simulation to be no more than qualitatively correct for  $x_1 > 0.5$ . In Figure 3 we have also included a comparison of the Darken approximation to  $D_{12,D}^K = x_1D_2 + x_2D_1$  with  $D_1$  and  $D_2$  from simulation. There is no significant deviation between  $D_{12}^K$  and  $D_{12,D}^K$  for neither methane – n-decane nor ethane – n-decane. Because one can obtain  $D_{12,D}^K$  ten times faster than  $D_{12}^K$  for a given statistical precision and because  $B_x$  represents the dominating error in the estimate of  $D_{12}$  one might as well use the Darken approximation to  $D_{12}$ .

The final point we will comment on is that if one compares the simulated thermal conductivities of ethane – n-decane and methane – n-decane with the Assael correlation one finds that the differences are never greater than the uncertainty.

#### 5 Conclusions

We have performed MD simulations of three mixtures of dissimilar molecules over the whole range of compositions, using simple one and two centre LJ model for the light components methane, ethane and CO<sub>2</sub> and the flexible AUA model for n-decane. The viscosities are always underpredicted with a maximum deviation of 30% at low gas content and a mean deviation of 16%. We found that neither the viscosity nor the thermal conductivity are very sensitive to the attractive cross interactions whereas all the diffusion coefficients are greatly affected. The diffusion coefficients are both under- and overestimated by up to 60%. The study has to a certain degree been able to separate three principal causes of the deviations: the imprecision of the pure n-decane potential, the steric size and shape effects and the effects of the attractive cross interactions. In sum, the potential models utilized seem both composition and property dependent, but the causes (and remedies) need to be further investigated.

# Acknowledgements

We thank Marc Durandeau for having initiated this work and for fruitful discussions. We would like to thank Total Exploration Production for a grant for one of us (DKD). We thank the Institut du Dévelopement et des Ressources en Informatique Scientifique (IDRIS) for a generous allocation of Cray T3E computer time.

# References

- W. D. Monnery, W. Y. Svrcek, and A. K. Mehrotra, Can. J. Chem. Eng. 73:3 (1995).
- [2] M. Helbaek, B. Hafskjold, D. K. Dysthe, and G. H. Sørland, J. Chem. Eng. Data 41:598 (1996).
- [3] W. Allen and R. L. Rowley, To be published in J. Chem. Phys. (1997).
- [4] D. K. Dysthe, A. H. Fuchs, and B. Rousseau, In preparation (1997).
- [5] P. Padilla and S. Toxvaerd, J. Chem. Phys. **94**:5653 (1991).
- [6] D. Möller, J. Oprzynski, A. Müller, and J. Fisher, Molec. Phys. 75:363 (1992).
- [7] K. Singer, A. Taylor, and J. V. L. Singer, Molec. Phys. 33:1757 (1977).
- [8] M. Wojcik, K. E. Gubbins, and J. G. Powles, *Molec. Phys.* 45:1209 (1982).
- [9] D. Fincham, N. Quirke, and D. J. Tildesley, J. Chem. Phys. 84:4535 (1986).
- [10] B. Y. Wang and P. T. Cummings, Molecular Simulation 10:1 (1993).
- [11] B. Rousseau and J.-M. Simon, In preparation (1997).
- [12] H. C. Andersen, J. Comput. Phys. **52**:24 (1983).
- [13] J.-M. Simon, D. K. Dysthe, A. H. Fuchs, and B. Rousseau, Submitted to Fluid Phase Equilibria (1997).
- [14] H. H. Reamer and B. H. Sage, Journal of Chemical and Engineering Data 7:161 (1962).
- [15] H. H. Reamer, R. H. Olds, B. H. Sage, and W. N. Lacey, Industrial and Engineering chemistry 34:1526 (1942).

- [16] B. Knapstad, P. A. Skjolsvik, and H. A. Øye, Ber. Bunsenges. Phys. Chem. 94:1156 (1990).
- [17] M. J. Assael, J. H. Dymond, M. Papadaki, and M. P. Patterson, *Int. J. Ther-mophys.* 13:659 (1992).
- [18] A. S. Cullick and M. L. Mathis, J. Chem. Eng. Data 29:393 (1984).
- [19] D. K. Dysthe, B. Hafskjold, J. Breer, and D. Čejka, J. Phys. Chem. 99:11230 (1995).

Table 1: Potential parameters.

|  | $\sigma_{ii}$<br>Å | $arepsilon_{ii} \ k_B \mathrm{K}$ | $m_i$ g mol $^{-1}$ | $\begin{matrix} I \\ \mathring{A}^2 g \ mol^{-1} \end{matrix}$ | $d_{	ext{bond}} \ 	ext{Å}$ |  |  |  |  |  |
|--|--------------------|-----------------------------------|---------------------|--|----------------------------|--|--|--|--|--|
| $CO_2$   | 3.035              | 163.3                             | 44                  | 43.124   | 2.37                       |  |  |  |  |  |
| $C_2H_6$   | 3.52               | 137.5                             | 30                  | 26.933   | 2.345                      |  |  |  |  |  |
| $\mathrm{CH}_4$  | 3.7327             | 149.92                            | 16                  | $d_{\scriptscriptstyle	ext{AUA}}$ $[	ext{Å}]$                  |                            |  |  |  |  |  |
| $\mathrm{CH}_3$  | 3.527              | 120                               | 15                  | 0.275  | 1.545                      |  |  |  |  |  |
| $\mathrm{CH}_2$  | 3.527              | 80                                | 14                  | 0.37   | 1.545                      |  |  |  |  |  |
| Bending potential, $u_{\theta} = (62543/2)(\cos \theta - \cos 114.6)^2 [k_B \text{K}]$ |                    |                                   |                     |  |                            |  |  |  |  |  |
| Torsion potential $u_t = \sum_{i=0} a_i \cos^i \chi [k_B K]$                           |                    |                                   |                     |  |                            |  |  |  |  |  |
| $a_0$  | $a_1$              | $a_2$                             | $a_3$               | $a_4$  | $a_5$                      |  |  |  |  |  |
| 1037.76  | 2426.07            | 81.64                             | -3129.46            | -163.28  | -252.73                    |  |  |  |  |  |
|  |                    |                                   |                     |  |                            |  |  |  |  |  |

Table 2: Simulation results of the n-decane + gas mixtures.

| n-C <sub>10</sub> | $x_1$         | ρ               | T     | P    | $\eta$                   | $\lambda$                             | $D_{12}^K$              | $D_1$                   | $D_2$                        |
|-------------------|---------------|-----------------|-------|------|--------------------------|---------------------------------------|-------------------------|-------------------------|------------------------------|
| +                 |               | $\rm kg~m^{-1}$ | K     | MPa  | $10^{-3} \mathrm{Pa\ s}$ | ${\rm W} {\rm \ m}^{-1} {\rm K}^{-1}$ | $10^{-9} \rm m\ s^{-1}$ | $10^{-9} \rm m\ s^{-1}$ | $10^{-9} \mathrm{m\ s^{-1}}$ |
| $\mathrm{CH_4}$   | 0.000         | 728.8           | 333.6 | 46.3 | 0.67                     | 0.15                                  |                         |                         | 1.85                         |
| 0114              | 0.093         | 720.6           | 328.4 | 44.0 | 0.48                     | 0.15                                  | 5.9                     | 7.04                    | 1.86                         |
|                   | 0.296         | 691.8           | 324.9 | 41.2 | 0.45                     | 0.13                                  | 5.5                     | 7.45                    | 2.22                         |
|                   | 0.500         | 644.1           | 330.5 | 45.5 | 0.23                     | 0.12                                  | 7.4                     | 10.44                   | 3.20                         |
|                   | 0.704         | 557.8           | 334.8 | 45.0 | 0.13                     | 0.11                                  | 9.0                     | 15.83                   | 4.81                         |
|                   | 0.907         | 375.1           | 326.8 | 39.4 | 0.058                    | 0.083                                 | 13.7                    | 30.9                    | 9.42                         |
|                   | 1.000         | 217.6           | 330.8 | 38.3 | 0.027                    | 0.062                                 |                         | 55.4                    |                              |
|                   |               |                 |       |      |                          |                                       |                         |                         |                              |
|                   |               |                 |       |      |                          |                                       |                         |                         |                              |
| $C_2H_6$          | 0.120         | 723.3           | 331.9 | 52.6 | 0.58                     | 0.15                                  | 4.7                     | 5.27                    | 1.86                         |
|                   | 0.398         | 683.2           | 334.6 | 48.4 | 0.36                     | 0.14                                  | 5.6                     | 7.08                    | 2.54                         |
|                   | 0.657         | 626.4           | 337.0 | 52.5 | 0.24                     | 0.13                                  | 6.3                     | 9.54                    | 3.54                         |
|                   | 0.870         | 538.2           | 330.9 | 47.6 | 0.14                     | 0.13                                  | 6.6                     | 13.2                    | 5.2                          |
|                   | 1.000         | 419.0           | 330.2 | 33.8 | 0.064                    | 0.10                                  |                         | 20.5                    |                              |
|                   |               |                 |       |      |                          |                                       |                         |                         |                              |
| CO                |               |                 |       |      |                          |                                       |                         |                         |                              |
| $CO_2$            |               |                 |       |      |                          |                                       |                         |                         |                              |
| $k_{ij}$          | 0.000         | 736.3           | 312.7 | 35.8 | 0.65                     | 0.15                                  |                         |                         | 1.48                         |
| 0.0               | 0.000 $0.148$ | 730.3           | 307.6 | 30.1 | 0.63                     | $0.15 \\ 0.15$                        | 5.0                     |                         | 1.40                         |
| $0.0 \\ 0.2$      | 0.148 $0.148$ | 744.9           | 314.9 | 42.1 | 0.63                     | $0.15 \\ 0.15$                        | 5.8                     |                         |                              |
| 0.2               | 0.148 $0.306$ | 753.4           | 306.2 | 21.5 | 0.03 $0.46$              | $0.13 \\ 0.14$                        | 4.9                     |                         |                              |
| $0.0 \\ 0.2$      | 0.306         | 753.4 $753.4$   | 314.5 | 42.2 | 0.46                     | 0.14                                  | 5.8                     |                         |                              |
| 0.2               | 0.500         | 774.1           | 333.5 | 50.9 | 0.40 $0.35$              | 0.14 $0.15$                           | 5.3                     |                         |                              |
| $0.0 \\ 0.2$      | 0.500         | 774.1           | 310.0 | 44.7 | 0.35 $0.40$              | 0.13 $0.14$                           | 5.8                     |                         |                              |
| 0.2               | 0.648         | 795.5           | 308.9 | 25.3 | 0.40 $0.25$              | 0.14                                  | 4.9                     |                         |                              |
| $0.0 \\ 0.2$      | 0.648         | 795.5<br>795.5  | 315.7 | 54.3 | 0.25                     | 0.13 $0.14$                           | 7.6                     |                         |                              |
| 0.2               | 0.048 $0.852$ | 837.7           | 305.4 | 16.9 | $0.25 \\ 0.17$           | 0.14                                  | 4.9                     |                         |                              |
| $0.0 \\ 0.2$      | 0.852         | 837.7           | 314.5 | 47.9 | 0.17                     | 0.13                                  | 6.8                     |                         |                              |
| 0.2               | 1.000         | 907.4           | 333.9 | 44.3 | 0.11                     | 0.13                                  | <b>0.</b> 0             |                         |                              |
|                   | 1.000         | 001.1           | 555.5 | 11.0 | 0.11                     | U.12                                  |                         |                         |                              |

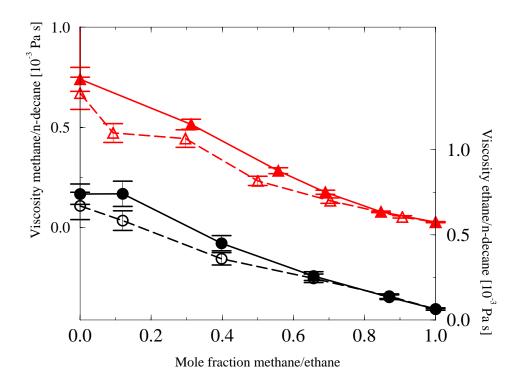


Figure 1: Viscosity in the methane/n-decane and the ethane/n-decane system as function of composition. Legends: triangles – methane/n-decane; circles – ethane/n-decane; open symbols – simulation; filled triangles – experimental; filled circles – experimental (pure fluids) and Assael correlation (mixture).

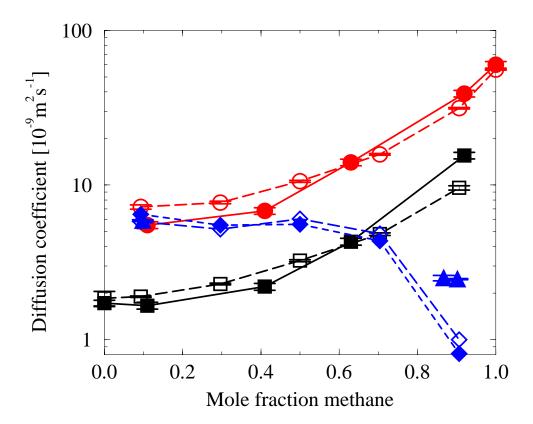


Figure 2: Diffusion in the methane/n-decane system as function of composition. Legends: open circles –  $D_{\text{methane}}$  from MD; filled circles –  $D_{\text{methane}}$  from experiment; open squares –  $D_{\text{decane}}$  from MD; filled squares –  $D_{\text{decane}}$  from experiment; open diamonds –  $D_{12} = B_x D_{12}^K$  from MD; filled diamonds –  $B_x D_{12}^K = B_x (x_1 D_2 + x_2 D_1)$  filled triangles – experimental  $D_{12}$ .

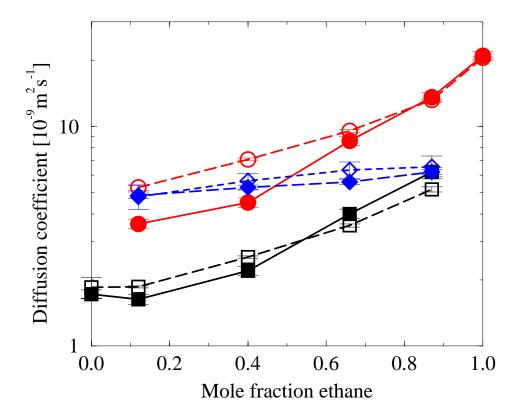


Figure 3: Diffusion in the ethane/n-decane system as function of composition. Legends: open circles –  $D_{\text{ethane}}$  from MD; filled circles –  $D_{\text{ethane}}$  from experiment; open squares –  $D_{\text{decane}}$  from MD; filled squares –  $D_{\text{decane}}$  from experiment; filled diamonds –  $D_{12}^K = x_1D_2 + x_2D_1$  from MD; open diamonds –  $D_{12}^K$  from MD.

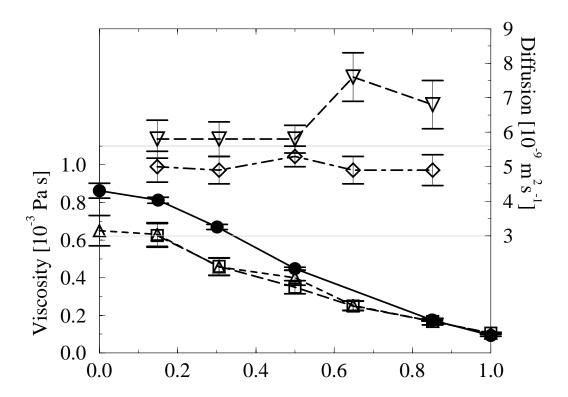


Figure 4: Viscosity and interdiffusion in the  $CO_2$ /n-decane system as function of composition. Legends: open squares – sim. viscosity with Lorentz-Berthelot mixing rules; triangle up – sim. viscosity with  $k_{ij} = 0.2$ ; filled circles – experiments. open diamonds – sim. interdiffusion with Lorentz-Berthelot mixing rules; triangle down – sim. interdiffusion with  $k_{ij} = 0.2$ ;